Received: 7 June 2017

DOI: 10.1002/mop.30943

Antipodal Vivaldi antennas with foldable hinged plates for adaptive polarization and gain adjustments

G. Byun[1] | T. H. Lim[2] | M. C. Kang[3] | H. Choo[2]

[1] Research Institute of Science and Technology, Hongik University, Seoul, South Korea

[2] School of Electronic and Electrical Engineering, Hongik University, Seoul, South Korea

[3] RF/Microwave Team, LIG Nex1, Yongin, South Korea

Correspondence
H. Choo, Research Institute of Science and Technology, Hongik University, Seoul, South Korea.
Email: hschoo@hongik.ac.kr

Abstract

This letter proposes a novel approach to adaptive polarization and gain adjustments for antipodal Vivaldi antennas using foldable hinged plates. The proposed antenna consists of upper and lower flared wings, and the wings are electrically extended using two rectangular plates. Metal hinges are then adopted to fold and unfold the plates, which allows the antenna to adjust the polarization in the entire range of the axial ratio and to further enhance the gain in the end-fire direction. Measured antenna characteristics demonstrate that the polarization and the gains are adaptively adjusted by varying the tilt angles of the hinged plates without a distortion of the broadband properties.

KEYWORDS

antipodal Vivaldi antenna, adaptive polarization, gain adjustment, hinged plates

1 | INTRODUCTION

Antipodal Vivaldi antennas (AVAs) have gained popularity because of their broad matching bandwidth, high gain, and the ease of fabrication.[1–4] In addition, their low profile properties allow for substantial use as array elements for beamforming applications,[5] such as radars and direction finding systems.[6,7] Generally, the accuracy and the reliability of such systems depend on the received signal strength (RSS) that can be significantly reduced by the polarization mismatch.[8] Although the polarization adjustable properties have been studied in Ref. [9] using microstrip patch antennas with parasitic elements, their narrow matching bandwidths are not suitable to maintain the strong RSS over a wide frequency range. In addition, the field of traditional broadband antenna engineering has mainly focused on the linear polarization without in-depth considerations of implementing other polarizations. Therefore, to maximize the RSS for broadband sources, there has been an increasing demand of accompanying the polarization adjustable properties with broadband antennas.

In this letter, we propose the design of novel AVAs with foldable hinged plates for adaptive polarization and gain adjustments. The proposed antenna consists of upper and lower wings printed on opposite sides of a thin dielectric

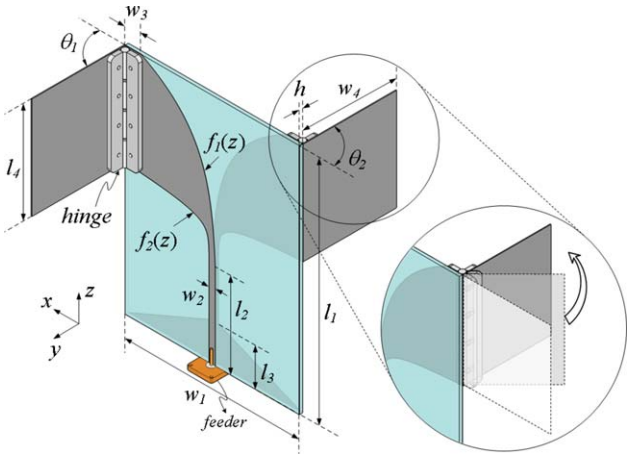

FIGURE 1 Geometry of the proposed AVA with foldable hinged plates. The adaptive adjustments of the polarization and gain can be accomplished by using parameters of θ_1 and θ_2. [Color figure can be viewed at wileyonlinelibrary.com]

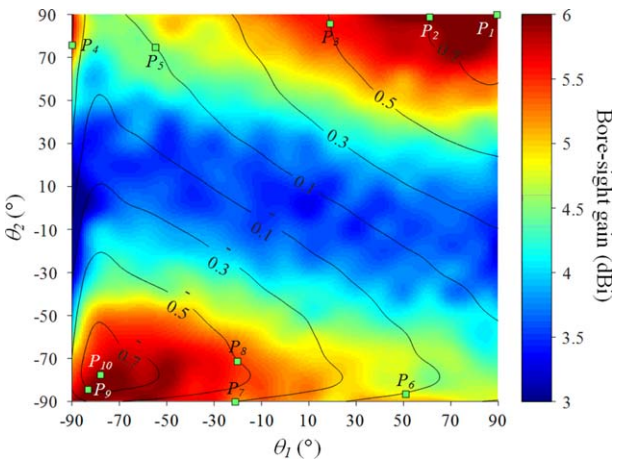

FIGURE 2 Effects of parameters θ_1 and θ_2 on the AR (contour) and the gain in the end-fire direction (color bar). [Color figure can be viewed at wileyonlinelibrary.com]

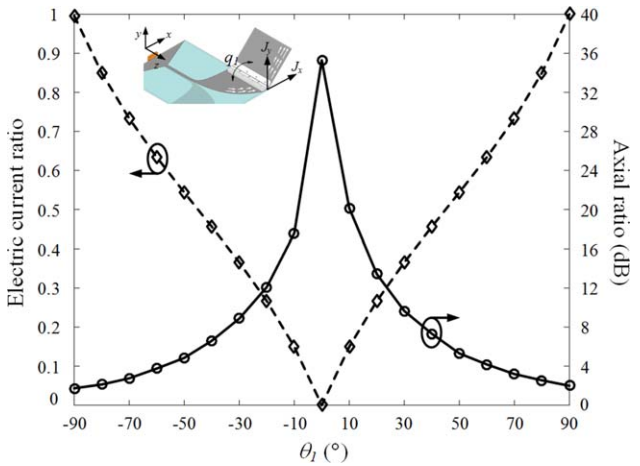

FIGURE 3 Analysis on the operating principle of the polarization adjustment in relation to the electric current ratio. [Color figure can be viewed at wileyonlinelibrary.com]

substrate, and the inner and outer edges of the wings are designed to flare according to predetermined exponential formulas for broad matching characteristics. These flared wings are then extended using rectangular plates at the top and bottom ends of the wings, and metal hinges are used to electrically connect and to fold the plates with a tilt angle varying from −90° to 90°. These hinged plates allow the antenna to adjust the polarization in the entire range of the axial ratios (ARs) including the linear polarization (LP), right-hand circular polarization (RHCP), left-hand circular polarization (LHCP), and even elliptic polarization (EP). Furthermore, by asymmetrically adjusting the tilt angle of each hinged plate, the proposed antenna can maximize the gain in the end-fire direction while maintaining desired ARs. Note that the AR can be controlled because the ratio of the vertical to horizontal components of the induced currents varies in accordance with the tilt angle. To verify the feasibility in terms of the polarization and the gain adjustments, the proposed antenna is fabricated, and its antenna characteristics are measured for each tilt angle in a full anechoic chamber. The results confirm that the polarization is adaptively adjusted in the entire range of the AR, and the gain can be further maximized without a distortion of the broadband characteristics.

2 | PROPOSED APPROACH

Figure 1 shows the geometry of the proposed antenna with the foldable hinged plates. The flared wings are printed on an FR4 substrate ($\varepsilon_r = 4.5$, $\tan\delta = 0.02$) with a width of w_1, a length of l_1, and a thickness of h. The shapes of their lower and upper edges are determined by two different exponential functions of $f_1(z)$ and $f_2(z)$, respectively. The width and length of the parallel strips used as twinline feeds are w_2 and l_2, and the shape of the balun is determined by parameter l_3. Then, each hinged plate is designed to have a width of w_4 and a length of l_4, and the tilt angles are adjusted using parameters of θ_1 and θ_2. In our structure, the width of the hinged plate (w_4) is designed to be about a half wavelength at the center of the operating frequency band, and the total aperture length, calculated as "$w_1 + 2w_4$," is determined to be approximately a half wavelength at the lowest operating frequency. The detailed parameters are tuned for the polarization and the gain adjustments in the frequency range from 1 to 6 GHz, and the optimized values are listed as follows: $w_1 = 70$ mm, $w_2 = 2.5$ mm, $w_3 = 6.5$ mm, $w_4 = 58$ mm, $l_1 = 133$ mm, $l_2 = 60$ mm, $l_3 = 11$ mm, $l_4 = 51.2$ mm, $h = 1.6$ mm, and the detailed formulas of the exponential curves are $f_1(z) = 0.001e^{\circ.4z}$ and $f_2(z) = 0.194e^{\circ.06z}$.

Figure 2 presents distributions of the AR and the gain in the end-fire direction according to θ_1 and θ_2, and the data are obtained from full-wave electromagnetic simulations by

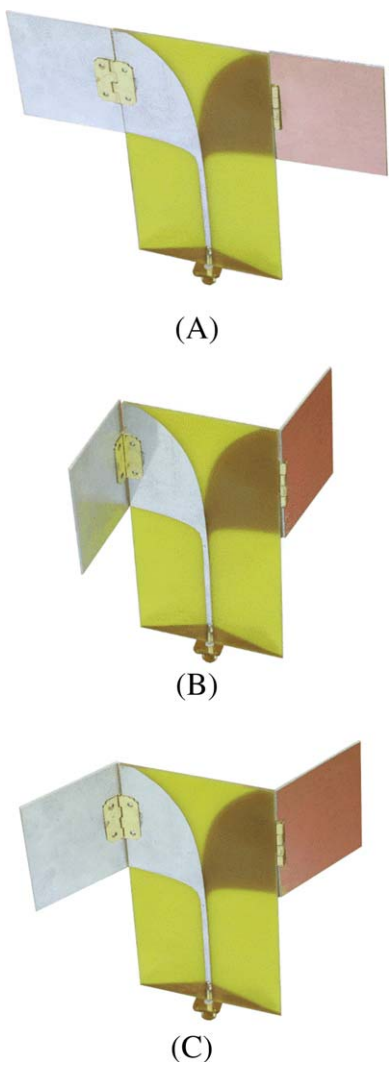

FIGURE 4 Photographs of the fabricated antennas. A, Linearly polarized antenna with $\theta_1 = \theta_2 = 0°$. B, Elliptically polarized antenna with $\theta_1 = \theta_2 = 45°$. C, Circularly polarized antenna with $\theta_1 = \theta_2 = 90°$. [Color figure can be viewed at wileyonlinelibrary.com]

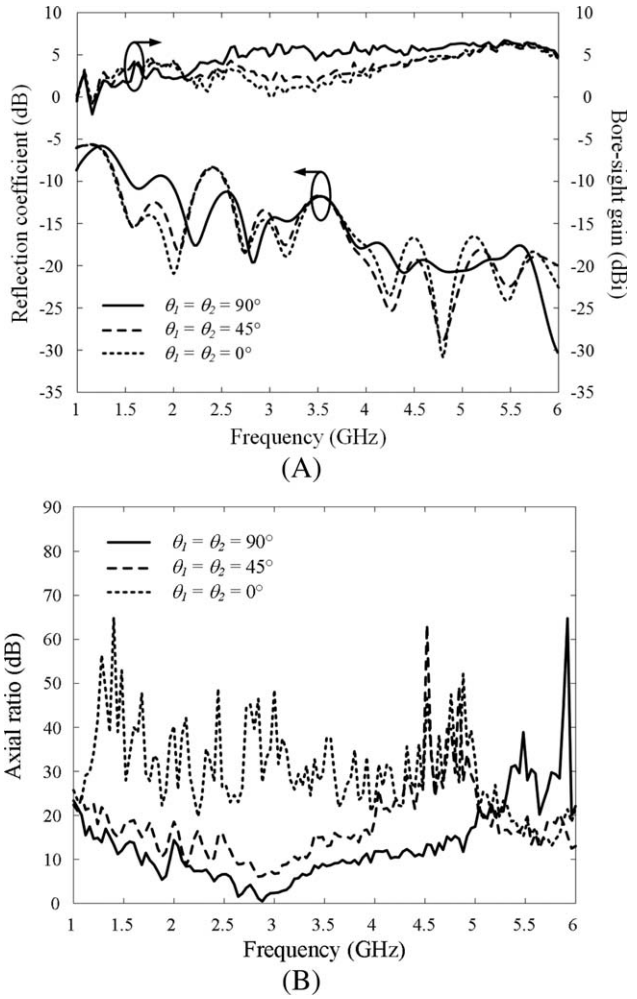

FIGURE 5 Performance comparisons of the fabricated antennas. A, Reflection coefficients and gain variations. B, Axial ratios according to frequency

varying the tilt angles from −90° to 90° at intervals of 1°. The results of the AR in contour lines demonstrate that the antenna is capable of varying the AR from 0.782 (P_1: $\theta_1 = 90°$, $\theta_2 = 90°$) to −0.797 (P_{10}: $\theta_1 = -77°$, $\theta_2 = -78°$), which includes the RHCP, LHCP, LP, and EP. The gain variations are specified by colors, and the square markers, denoted as P_2, P_3, P_4, …, P_9, indicate the maximum gains for fixed ARs of 0.7, 0.5, 0.3, …, −0.7, respectively. As can be seen, the maximum gains for the given ARs are not diagonally distributed, which implies that the asymmetric adjustment of the tilt angle is required for each hinged plate for the gain improvement. For example, when the antenna has the AR of 0.5, the maximum gain of 5.6 dBi appears at P_3 with coordinates of $\theta_1 = 19°$ and $\theta_2 = 86°$. This is because the phases of the electric currents induced in the upper and lower wings are slightly off the center due to the substrate thickness and the balun attached to the lower wing, and these deviated phases should be compensated for the maximized gains by asymmetrically adjusting θ_1 and θ_2. To analyze the operating principle of the polarization adjustment, we observe the electric current densities induced on the flared wings and the hinged plates using the full-wave simulations. The *x*-component and *y*-component of the simulated results are denoted as J_x and J_y in the inset figure of Figure 3, and the ratios calculated as $|J_y|/|J_x|$ are compared to ARs by varying the value of θ_1. When θ_1 is equal to 0°, the value of $|J_y|$ approaches to zero, and the antenna is linearly polarized with an AR of 35.3 dB. As the absolute value of θ_1 increases, the ratio of $|J_x|$ to $|J_y|$ becomes close to one, which results in the circular polarization with an AR less than 3 dB. These results show that the observation of the electric current ratio well represents the operating principle of the proposed structure.

3 | FABRICATION AND MEASUREMENT

Figure 4 shows photographs of the fabricated AVA with the foldable hinged plates, and their impedance matching and radiation characteristics are measured in a full anechoic chamber to verify the feasibility. In this verification, the tilt angles of θ_1 and θ_2 are symmetrically adjusted for 0°, 45°, and 90° to achieve the LP, EP, and RHCP with ARs of 0.01, 0.49, and 0.78, respectively. Figure 5A presents the measured reflection coefficient and the gain in the end-fire direction as a function of frequency. The solid, dashed, and dotted lines indicate the results of the AVAs with the LP, EP, and RHCP. These results demonstrate that the adjustment of the tilt angles does not affect the impedance matching characteristics with similar 10-dB matching bandwidths of 4.6 GHz (LP, 1.4–6 GHz), 4.6 GHz (EP, 1.4–6 GHz), and 4.5 GHz (RHCP, 1.5–6 GHz). Figure 5B shows a comparison of the measured ARs in the end-fire direction, and the measured values tend to decrease as the tilt angles become greater. For example, the measured values at 3 GHz decrease gradually from 48.5 dB (LP) to 6.8 dB (EP), and eventually to 2.4 dB (RHCP). These results demonstrate the polarization properties of such broadband AVAs can be flexibly adjusted in the entire AR range by folding or unfolding the hinged plates.

Figure 6 shows measured radiation patterns in comparison with simulated results. The solid and dashed lines indicate measured and simulated circular polarization gains in dBic for RHCP, and the dotted and dash-dotted lines present cross-polarization gains, which is the LHCP. The measured half-power beamwidths (HPBWs) of the copolarization patterns are 104.6°, 70.5°, and 50.4° in the *zx*-plane, and the HPBWs in the *yz*-planes are 104.1°, 111.4°, and 81.6° for the AVAs with the LP, EP, and RHCP, respectively. Due to the polarization adjustment, the cross-polarization level in the bore-sight direction of $\theta = 0°$ is decreased from −3 dB ($\theta_1 = \theta_2 = 0°$) to −7.5 dB ($\theta_1 = \theta_2 = 45°$) and becomes even lower with a value of −12.7 dB in case of $\theta_1 = \theta_2 = 90°$. These results confirm that the foldable hinged plates allow the AVAs to adjust the polarization properties without serious pattern distortions.

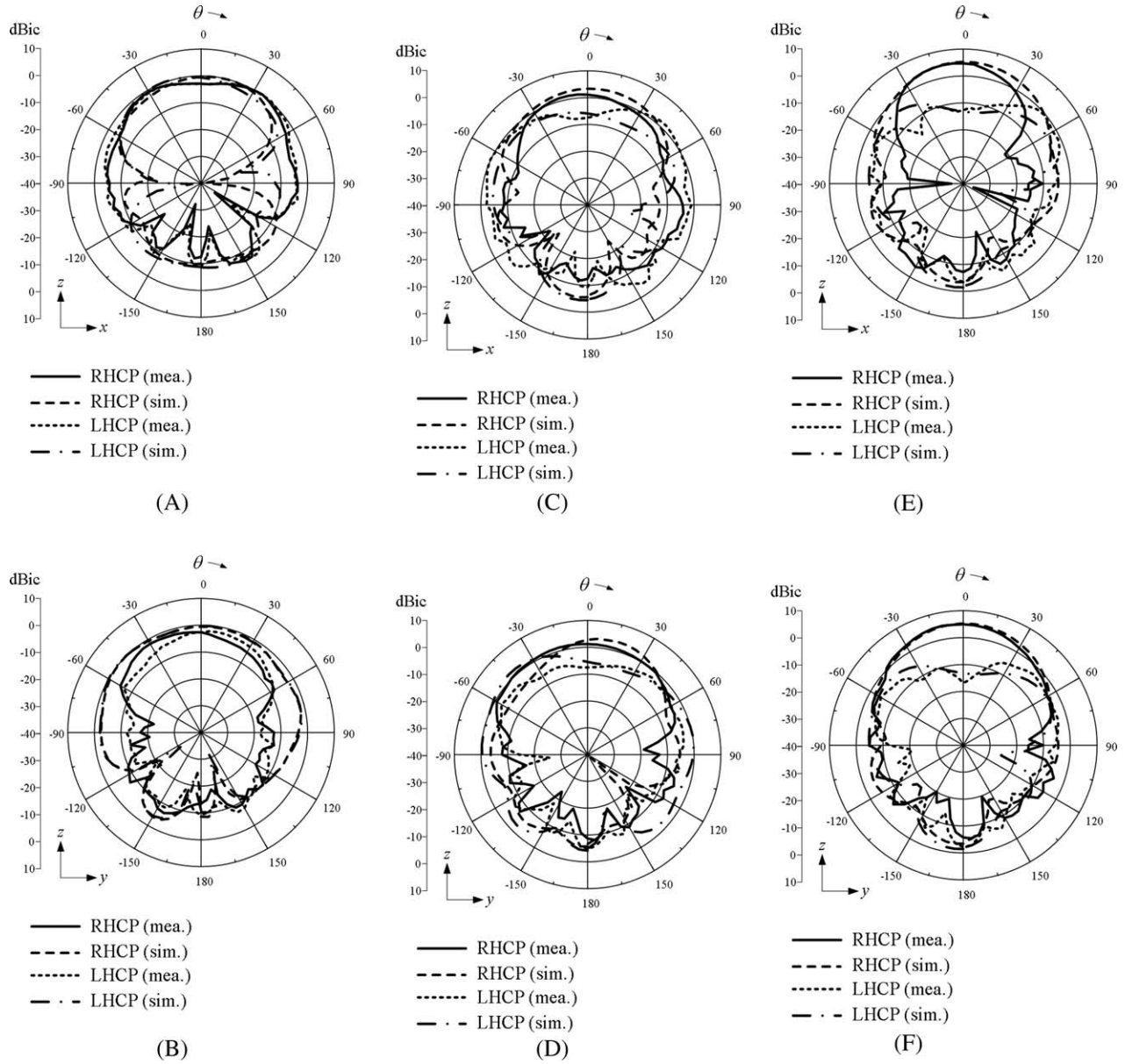

FIGURE 6 2D radiation patterns of the fabricated antennas. A, *zx*-plane ($\theta_1 = \theta_2 = 0°$). B, *zy*-plane ($\theta_1 = \theta_2 = 0°$). C, *zx*-plane ($\theta_1 = \theta_2 = 45°$). D, *zy*-plane ($\theta_1 = \theta_2 = 45°$). E, *zx*-plane ($\theta_1 = \theta_2 = 90°$). F, *zy*-plane ($\theta_1 = \theta_2 = 90°$)

4 | CONCLUSIONS

We proposed the novel approach to adaptive polarization and gain adjustments for AVAs using the foldable hinged plates. By varying the tilt angles of the hinged plates, the polarization could be changed in the entire range of the AR, and the gain in the end-fire direction was further enhanced for any desired AR by asymmetrically adjusting the tilt angle of each hinged plate. The proposed antenna was fabricated, and the feasibility of the polarization and gain adjustments was verified through measurements. The fabricated antenna showed measured ARs of 48.5, 6.8, and 2.4 dB at tilt angles of 0°, 45°, and 90°, respectively, at 3 GHz. The results confirmed that the foldable hinged plates provided new features of the polarization and gain adjustments, and the broadband properties were maintained with 10-dB matching bandwidths of greater than 4.5 GHz.

ACKNOWLEDGMENTS

This research was supported by Civil Military Technology Cooperation (CMTC) and the Basic Science Research Program through the National Research Foundation of Korea (NRF) funded by the Ministry of Education (No. 2015R1A6A1A03031833).

ORCID

H. Choo http://orcid.org/0000-0002-6357-2634

REFERENCES

[1] Gazit E. Improved design of the Vivaldi antenna. *IEE Proc Microwave Antennas Propag.* 1988;135:89–92.

[2] Bourqui J, Okoniewski M, Fear EC. Balanced antipodal Vivaldi antenna with dielectric director for near-field microwave imaging. *IEEE Trans Antennas Propag.* 2010;58:2318–2326.

[3] Nassar IT, Weller TM. A novel method for improving antipodal Vivaldi antenna performance. *IEEE Trans Antennas Propag.* 2015;63:3321–3324.

[4] Manteghi M, Rahmat-Samii Y. A novel UWB feeding mechanism for the TEM horn antenna, reflector IRA, and the Vivaldi antenna. *IEEE Antennas Propag Mag.* 2004;46:81–87.

[5] Dyadyuk V, Stokes L, Nikolic N, Weily AR. Planar directional beam antenna design for beam switching system applications. *J Electromagn Eng Sci.* 2017;17:14–19.

[6] Langley JDS, Hall PS, Newham P. Balanced antipodal Vivaldi antenna for wide bandwidth phased arrays. *IEE Proc Microwave Antennas Propag.* 1996;143:97–102.

[7] Loui H, Weem JP, Popovic Z. A dual-band dual-polarized nested Vivaldi slot array with multilevel ground plane. *IEEE Trans Antennas Propag.* 2003;51:2168–2175.

[8] Muehldorf EI, Teichman MA, Kramer E. Polarization mismatch errors in radio phase interferometers. *IEEE Trans Aerosp Electron Syst.* 1972;AES-8:135–141.

[9] Byun G, Choo H. Antenna polarisation adjustment for microstrip patch antennas using parasitic elements. *Electron Lett.* 2015;51:1046–1048.

How to cite this article: Byun G, Lim TH, Kang MC, Choo H. Antipodal Vivaldi antennas with foldable hinged plates for adaptive polarization and gain adjustments. *Microw Opt Technol Lett*. 2017;60:183–187. https://doi.org/10.1002/mop.30943

Received: 7 June 2017

DOI: 10.1002/mop.30942

Demonstration of negative refractive index with low-cost inkjet-printed microwave metamaterials

Hande İbili | **Barışcan Karaosmanoğlu** | **Özgür Ergül**

Electrical and Electronics Engineering Department, Middle East Technical University, Ankara, Turkey

Correspondence
Hande İbili, Electrical and Electronics Engineering Department, Middle East Technical University, Ankara, Turkey.
Email: bariscan@metu.edu.tr

Abstract

We present low-cost fabrications of inkjet-printed metamaterials that are resonating at microwave frequencies. A very low-cost setup involving commercial desktop printers loaded with silver-based inks is constructed and used to fabricate the metamaterials. We show that, despite the challenges in the low-cost fabrication processes, successful prints, and metamaterial samples can be obtained. A composite metamaterial design, which possesses a bandlimited transparency due to the induced negative refractive index, is fabricated and tested to demonstrate the feasibility of low-cost metamaterials with relatively complex geometries involving three-dimensional arrangements.

KEYWORDS

metamaterials, negative refractive index, microwave applications

1 | INTRODUCTION

Inkjet-printing technology has become an interesting and important alternative to conventional manufacturing processes for the fabrication of low-cost electronic devices, such as antennas,[1,2] microwave components and filters, as well as general frequency-selective surfaces[3] and absorbers.[4] In addition to special material printers designed and used particularly for this purpose, it is possible to construct very low-cost setups[5] involving standard desktop printers loaded with conductive inks for successfully printing usable devices. While being inexpensive, these inkjet-printed components are also disposable, flexible, and easy to replicate. As a drawback, the low-cost fabrication process must be carefully designed by considering the printer, paper, and ink types.[6] In addition, a separate temperature curing, which also needs to be optimized, must follow each printing session.

In this contribution, we demonstrate the design and fabrication of three-dimensional microwave metamaterials using a very low-cost inkjet-printing setup as described above. We particularly demonstrate an interesting phenomenon of negative refractive index using a block of metamaterial with less than 1 USD cost (including printer). Using only two-dimensional prints produced by standard desktop printers makes the fabricated metamaterials unique and different from those produced by special material (including three-dimensional) printers. In addition, our focus is composite metamaterials, needing three-dimensional arrangement of